Simulation and Experimental Analysis of Pulse Tube Refrigerator with an Active Phase Controller

S. Yang, Y. N. Wu, Z. P. Zhou, Z. H. Jiang, A. K. Zhang

Shanghai Institute of Technical Physics
Chinese Academy of Sciences
Shanghai, 200083, P. R. China

ABSTRACT:

The pulse tube refrigerator (PTR) with an active phase controller (APC) is a novel type of pulse tube refrigerator, where the inertance tube and the reservoir are replaced by an APC. In this study, a numerical analysis of a PTR with an APC was performed using a two-dimensional axisymmetric Computational Fluid Dynamics (CFD). The influences of the phase and swept volume of APC on phase, mass flow rate, pressure ratio and the performance of PTR are discussed. Some experiments are carried out to validate the numerical results.

INTRODUCTION

As illustrated in Figure 1, in the PTR, the displacer piston (as found in the Stirling and Gifford-McMahon (GM) regenerative systems) is eliminated, the cold moving parts have been replaced by stationary components (orifice or inertance tube). In pulse tube refrigerators with small cooling capacity, the inertance tube cannot shift the phase between the mass flow and pressure to the ideal angle because of the low acoustic power at the inlet of the inertance tube[1-2]. In addition, the acoustic power is absorbed and dissipated into waste heat in the inertance tube, which causes a decrease in the efficiency of the PTR[3].

A key component to create a more efficient PTR is the phase shifter[4], which controls the phase shift between the mass flow and the pressure. In this study, a linear compressor, which is directly connected at the warm end of the pulse tube using a connecting tube, is used as a phase shifter (Figure 2)[5-6].

Figures 2 and 3 show an electrical analogy model of the pulse tube refrigerator with an inertance tube or APC. In this model, the pressure wave generator (PWG) and the active phase controller (APC) are analogous to electric motors, the regenerator is analogous to an electric resistance and the inertance and the reservoir are analogous to an electric capacity and electrical ground[7-8].

Comparing these two electrical analogy models of the pulse tube refrigerator with an inertance tube or APC, the advantage of the active phase controller pulse tube (APCPTR) is the convenience of controlling the phase between the pressure and the mass flow in the PTR. In addition, when the hot end of the regenerator and the back of the APC are connected to recover power from the gas in the hot end of the pulse tube, the system efficiency can be increased.

Cryocoolers 19, edited by S.D. Miller and R.G. Ross, Jr.

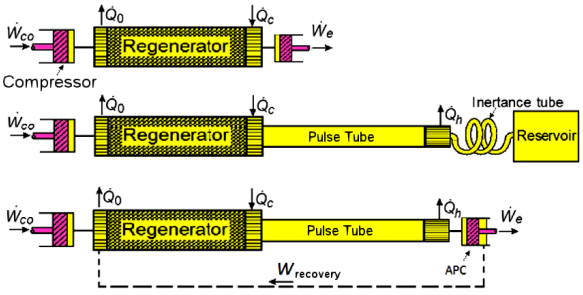

Figure 1. Schematic of three different configurations of cryocooler based on Stirling cycle

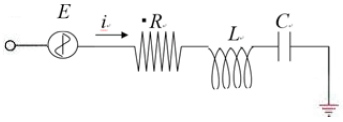

Figure 2. Electrical analogy of pulse tube refrigerator with inertance tube

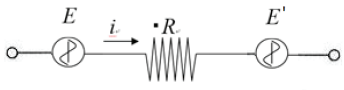

Figure 3. Electrical analogy of pulse tube refrigerator with APC

SIMULATION MODEL

In this study, FLUENT®, CFD modelling software, is employed to simulate the flow of fluid and the pressure distribution in the pulse tube refrigerator[9]. All of the details of modeling and meshing of the 2-D axis-symmetric pulse tube refrigerator model is done using the modeling software GAMBIT®. In FLUENT®, the conservation equations of mass, momentum and velocity are solved using a finite volume method. There are several turbulence models available in the code. The flow was calculated by the SIMPLE® method, and a second order upwind differential scheme was applied for the approximation of the convective terms. The implemented mesh involved about 350,000 cells (Figure 2).

A complete pulse tube refrigerator using a linear compressor as a phase controller consists of the compressor (1), the transfer line (2), the aftercooler (3), the regenerator (4), the cold-end heat exchanger (5), the pulse tube (6), the hot-and heat exchanger (7), the connecting tube (8), and the active phase controller (9) (see Figure 4).

The governing equations of Fluent® used to solve the mass, momentum, and energy for the working medium in this computational model are:

$$\frac{\partial \rho}{\partial t} + \nabla \cdot (\rho V) = 0 \tag{1}$$

$$\rho \frac{D\vec{v}}{Dt} = -\rho g \vec{n} - \nabla \vec{P} + \nabla \cdot \left\{ \mu \left[(\nabla \vec{v} + \nabla \vec{v}^{t}) - \frac{2}{3} \nabla \cdot \vec{v} I \right] \right\} \tag{2}$$

$$\rho c \left[\frac{\partial T}{\partial t} + (\vec{v} \cdot \nabla) T \right] = \nabla \cdot (k \nabla T) \tag{3}$$

The compressor and the APC are modeled using dynamic mesh. A User Defined Function (UDF) is written to track the motion of the pistons with respect to time.

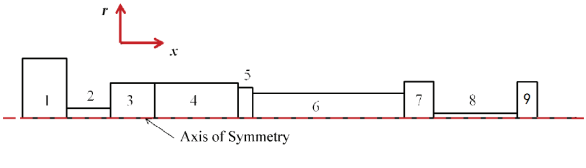

Figure 4. Schematic of the simulation model

The regenerator and the heat exchangers are modeled as porous regions; their viscous loss and the inertial loss are considered. In Fluent®, porous media are modeled by the addition of a momentum source term to the standard fluid flow equations. The source term is composed of two parts: a viscous loss term and an inertial loss term.[10-11]

$$s_i = -\left\{\sum_{j=1}^{3} D_{ij} u v_j + \sum_{j=1}^{3} C_{ij} \frac{1}{2} \rho |v| v_j\right\} \quad (4)$$

where s_i is the source term for the i the (x, y or z) momentum equation, $|v|$ is the magnitude of the velocity and D and C are prescribed matrices. This momentum sink contributes to the pressure gradient in the porous cell, creating a pressure drop that is proportional to the fluid velocity (or velocity squared) in the cell.

$$s_i = -\left\{\frac{\mu}{\alpha} v_i + C_2 \frac{1}{2} \rho |v| v_i\right\} \quad (5)$$

where α is the permeability and C_2 is the inertial resistance factor, simply specify D and C as diagonal matrices with $\frac{1}{\alpha}$ and C_2, respectively, on the diagonals (and zero for the other elements).

In the regenerator, the thermal conductivity and specific heat capacity of material are only functions of temperature.

The working fluid, helium, is modeled as an ideal gas; its viscosity and thermal conductivity are only functions of temperature.

The warm-end heat exchanger and the aftercooler are set to a constant temperature of 300K.

The working frequency of this PTR is 50 Hz. In this simulation, the time step of this transient model is 0.0002 second.

RESULTS AND DISCUSSION

Velocity in two kinds of pulse tube refrigerator in one cycle

In this study, a numerical simulation of 2 different PTRs were performed to identify the differences between a PTR with APC and a PTR with inertance tube. In the simulation, the swept volume of the piston of the PWG is 4.53 x 10^{-6} m^3, the swept volume of the APC is changing from 1.0625 x 10^{-6} m^3 to 3.1875 x 10^{-6} m^3, the phase between PWG (Pressure Wave Generator) and APC is changing from 70°to 140°(PWG-APC), and the temperature of cold heat exchanger is fixed at 100K.

Figures 5 and 6 show the flow of helium in the pulse tube refrigerator with an inertance tube and the pulse refrigerator with APC in one cycle. The CFD analysis shows that the APC which controls the phase between the mass flow and the pressure by changing the phase and the swept volume of APC can replace the inertance tube.[2]

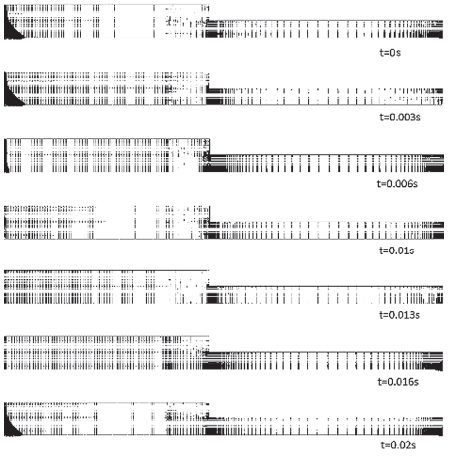

Figure 5. Snapshot of velocity vectors in pulse tube refrigerator with APC in one cycle

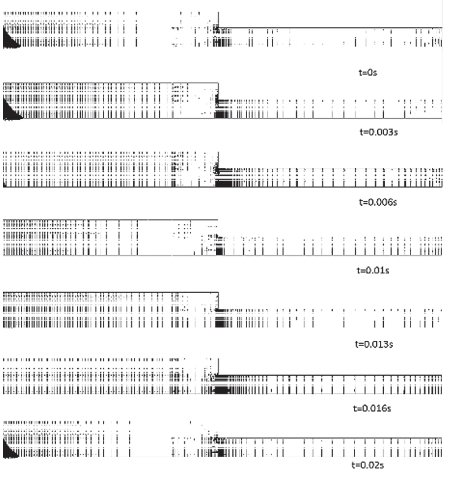

Figure 6. Snapshot of velocity vectors in pulse tube refrigerator with inertance tube in one cycle

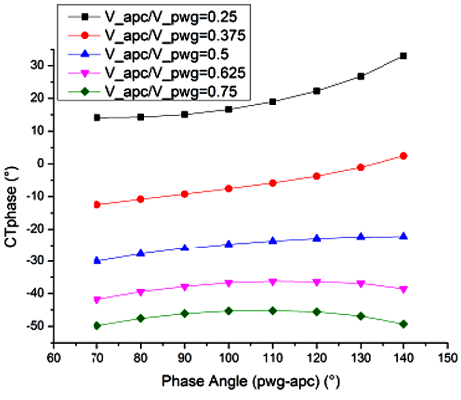

Figure 7. CT phase versus phase between PWG and APC

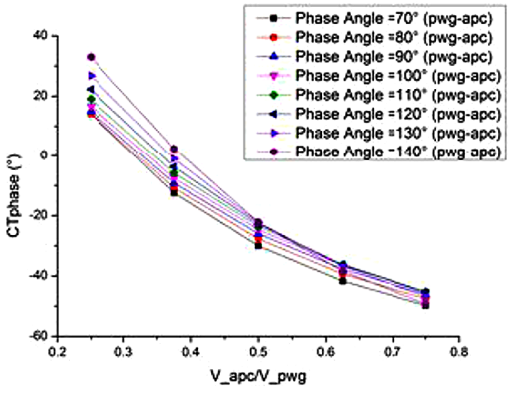

Figure 8. CT phase versus Vapc/Vpwg

Phase between the Pressure and the Axial Velocity (CTphase) at the Cold End of PTR

Figure 7 shows the phase between the pressure and the axial velocity at the cold end of PTR and the phase between PWG and APC are strongly correlated. Figure 8 shows the phase between the pressure and the axial velocity at the cold end of the pulse tube and swept volume of PWG and APC are strongly correlated. With the increase of the swept volume in APC, the phase between the pressure and the axial velocity at the cold end of the pulse tube is reduced.

Both swept volume and phase of the PWG and the APC have a great influence on the phase between the pressure and the axial velocity, the swept volume of APC plays a more important role in it.

Mass Flow Rate (Mc) at the Cold End of PTR

Figure 9 shows mass flow rate at the cold end of the pulse tube and the phase angle between the pistons in the compressor and the APC are strongly correlated. With the increase of the phase between the compressor and APC, the mass flow rate at the cold end of the pulse tube is reduced.

Figure 10 shows the phase between the pressure and the axial velocity at the cold end of the pulse tube and swept volume of two pistons are strongly correlated. With the increase of the swept volume in APC, the phase between the pressure and the axial velocity at the cold end of the pulse tube is increased.

Both swept volume and phase of the compressor and APC play a great influence on the phase between the pressure and the axial velocity; there exists an optimum phase angle between the two pistons and the optimum swept volume of the two pistons.

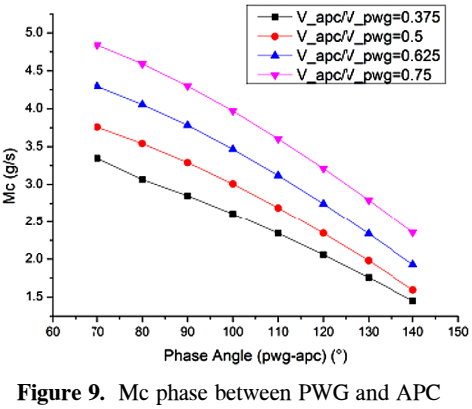

Figure 9. Mc phase between PWG and APC

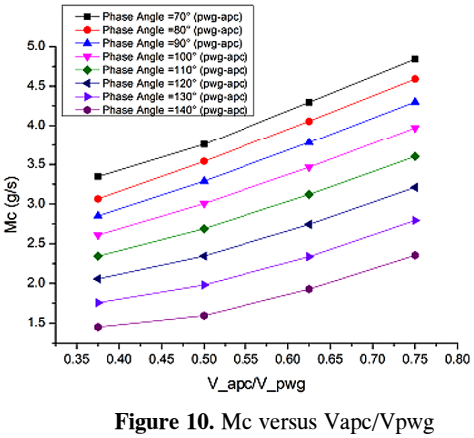

Figure 10. Mc versus Vapc/Vpwg

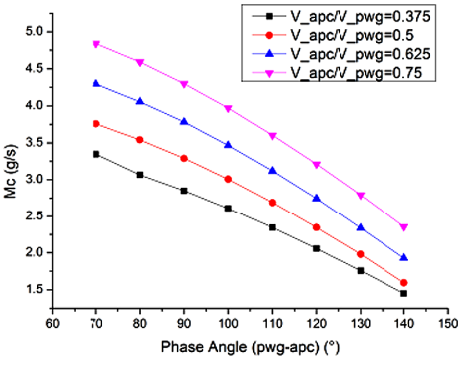

Figure 11. CTPr versus phase between PWG and APC

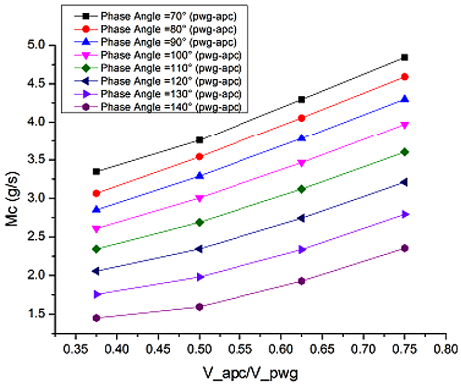

Figure 12. CTPr versus Vapc/Vpwg

Pressure Ratio at the Cold End of the Pulse Tube (CTPr)

Figure 11 shows the pressure ratio at the cold end of the pulse tube and the phase angle between the pistons in the compressor and the APC are strongly correlated. With the increase of the phase between the compressor and APC, the pressure ratio at the cold end of the pulse tube is increased.

Figure 12 shows the pressure ratio at the cold end of the pulse tube varying the swept volume of the APC. With an increase in the swept volume of the APC, the pressure ratio at the cold end of the pulse tube is increased. The increase in the pressure ratio at the cold end of the pulse tube produces an increase of the efficiency. With an increase in the swept volume in APC, the power supply increases. There exists an optimum phase angle between the two pistons and the optimum swept volume of the two pistons.

The simulation shows that the active phase controller can be applied to pulse tube refrigerators that have low acoustic power at the warm end, by changing the phase and the swept volume of compressor and APC.

Cooling Capacity (Qc) of PTR with APC

Figure 13 shows that the cooling capacity of the PTR with APC and the phase between the PWG and APC are strongly correlated; there exists an optimum phase for highest Qc.

Figure 14 shows the cooling capacity of the PTR with APC varying the swept volume of APC. With the increase of the swept volume of APC, the cooling capacity of the PTR is increased. With the increase of the swept volume in APC, the power supply increased as well; there exists an optimum phase and an optimum swept volume of the PWG and APC.

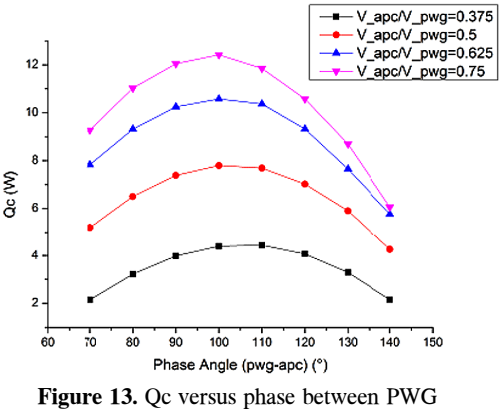

Figure 13. Qc versus phase between PWG and APC

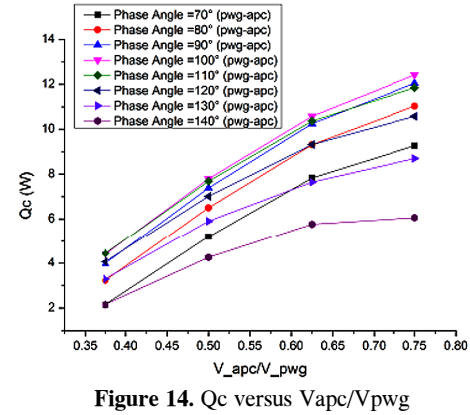

Figure 14. Qc versus Vapc/Vpwg

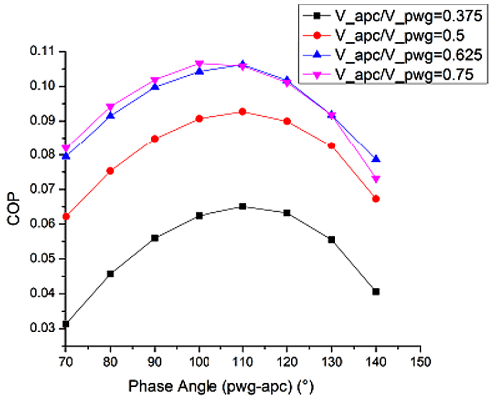

Figure 15. COP versus phase between PWG and APC

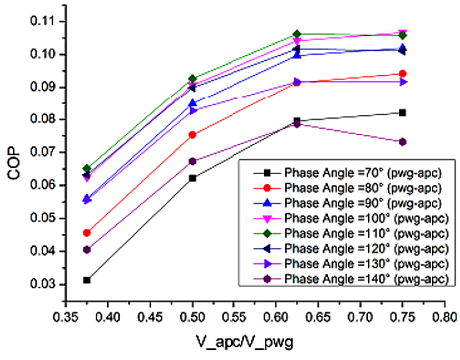

Figure 16. COP versus Vapc/Vpwg

COP of PTR with APC

Figures 15 and 16 show that as the phase angle between the PWG and the APC increases, the COP increases until the phase angle reaches a certain value. There exists an optimum phase and an optimum swept volume for the PWG and APC.

The quantity of cooling capacity depends on the phase between the pressure and the axial velocity, the mass flow rate and the pressure ratio at the cold end of the pulse tube. The COP of PTR depends on the cooling capacity and the PV power supplied by the PWG.

$$Q_c \propto \langle \dot{W} \rangle_t = \langle P\dot{V} \rangle_t = \frac{1}{2}|P||\dot{V}|\cos\theta \tag{6}$$

The simulation shows that, the phase and swept volumes of PWG and APC play an important influence on the phase angle of the phase between the pressure and the axial velocity at the cold heat exchanger of the pulse tube.

Experimental Setup

A photograph of the experimental setup is shown in Figure 17. The left side compressor is used as the pressure wave generator (PWG) and the right side compressor is used as the active phase controller (APC). The APC is directly connected to the warm end of the pulse tube using a stainless steel tube.

As shown in the schematic in Figure 18, the PWG and the APC are operated by amplifified electric signals from a function generator. The power supply of the PWG and the APC consists of two power amplifiers. The phase angle between the PWG and APC is dominated by the signal generator. The displacement transducers are used to measure the displacement of the piston in PWG and APC.

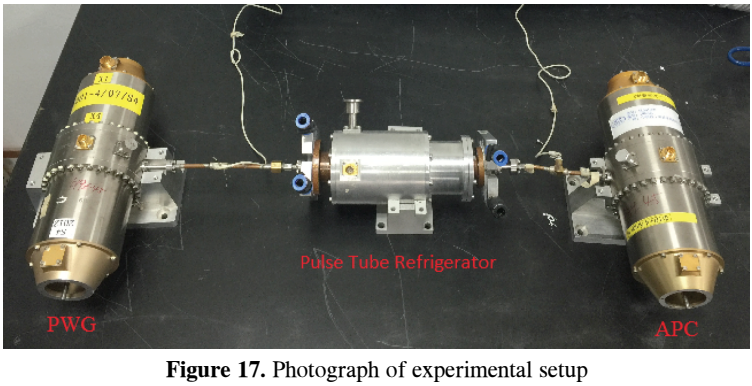

Figure 17. Photograph of experimental setup

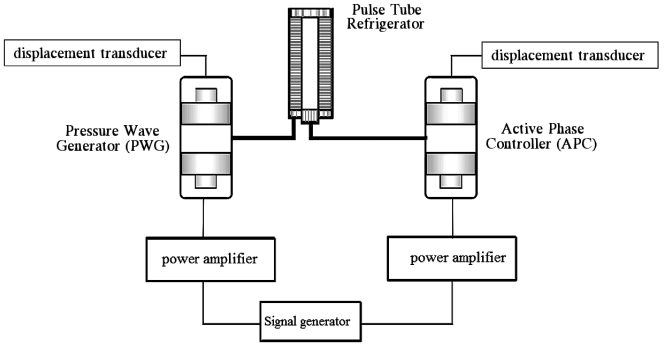

Figure 18. Schematic of experimental setup

All the experiments have been carried out at an operating frequency of 50 Hz and an initial charging pressure of helium gas of 3.2 MPa. The warm-end heat exchanger and the aftercooler are set to a constant temperature of 300 K. These experimental results are shown as follows.

EXPERIMENTAL RESULTS

Carnot Efficiency of PTR with APC

In this experiment, all the experiments have been carried out at an operating frequency of 50 Hz and an initial charging pressure of helium gas of 3.2 MPa. The warm-end heat exchanger and the aftercooler are set to a constant temperature of 300 K. The initial input power of the compressor of the PWG was 120 W, and the initial input power of the compressor of the APC was 15.5 W. The cold end temperature was fixed at 100 K.

Figure 19 shows the phase PWG and APC by varying the COP of the pulse tube refrigerator. The highest COP is 1.05×10^{-2}, when the phase angle between the PWG and APC is 110° (PWG-COP). The predicted performance of the PTR is in reasonable agreement with the experimental data.

No-Load Temperature of PTR with APC

In this experiment, all the experiments have been carried out at an operating frequency of 50 Hz and the initial charging pressure of helium gas is 3.2 MPa. The warm-end heat exchanger and the aftercooler are set to a constant temperature of 300 K. The amplitude of the compressor is 8 mm, and the amplitude of the APC is changed from 2 mm to 7 mm.

Figure 20 shows the temperature at the cold heat exchanger of the pulse tube refrigerator without a thermal load; the lowest temperature is 75.5 K, when amplitude of the APC was 7 mm. The predicted performance of the pulse tube refrigerator is in reasonable agreement with the experimental data.

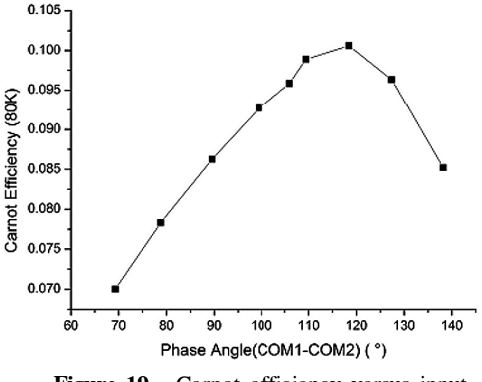

Figure 19. Carnot efficiency versus input power of PWG and APC

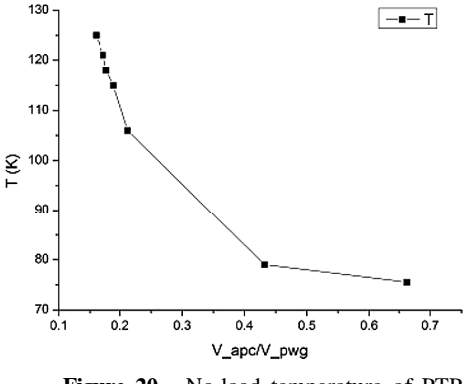

Figure 20. No-load temperature of PTR with APC versus V_{apc} / V_{pwg}

CONCLUSION

In this study, a numerical model of Stirling type pulse tube refrigerator with an active phase controller was performed using a two-dimensional axis-symmetric CFD. The influences of the phase and swept volume of the APC on the phase, mass flow, pressure ratio and the performance of PTR are discussed. The predicted performance of the pulse tube refrigerator is in reasonable agreement with the experimental data.

1. The Stirling type pulse tube refrigerator with the active phase controller has been experimentally investigated.
2. The investigations have demonstrated the capability of CFD models to predict the performance and discover the losses in the pulse tube refrigerator.
3. There exist an optimum phase between two pistons and the optimum swept volume of two pistons for the PTR to improve system efficiency.

ACKNOWLEDGMENTS

This work was supported by the Natural Science Foundation of Shanghai (NO. 16ZR1441500).

REFERENCES

1. Hu, J.Y., Ren, J., Luo, E.C. and Dai, W.,. "Study on the Inertance Tube and Double-inlet Phase Shifting Modes in Pulse Tube Refrigerators," *Energy Conversion and Management*, 52(2) (2011), pp. 1077-1085.
2. Antao, D.S., Farouk, B., "Numerical and Experimental Characterization of the Inertance Effect on Pulse Tube Refrigerator Performance," *International Journal of Heat and Mass Transfer*, 76 (2014), pp. 33-44.
3. Swift, G.W., Gardner, D.L., Backhaus,S., "Acoustic recovery of lost power in pulse tube refrigerators," *Journal of the Acoustical Society of America*, 105(2) (1999), pp. 711-724.
4. Li, Z., Gan, Z. and Qiu, L., "Cold Inertance Tube for 4 K Stirling Type Pulse Tube Cryocoolers," P*hysics Procedia*, 67 (2015), pp. 451-455.
5. Brito, M., Peskett, G., "Numerical Model of Free Warm Expander Pulse Tube Cooler," *Cryogenics*, 41(10) (2001), pp. 751-755.
6. Brito, M., Peskett, G., "Experimental Analysis of Free Warm Expander Pulse Tube," *Cryogenics*, 41(10) (2001), pp. 757-762.
7. Riley, P.H., "Towards a Transient Simulation of Thermo-acoustic Engines Using an Electrical Analogy," *Procedia Engineering*, 56 (2013), pp. 821-828.
8. Bailly, Y., Nika, P., "Comparison of Two Models of a Double Inlet Miniature Pulse Tube Refrigerator: Part B Electrical Analogy," *Cryogenics*, 42(10) (2002), pp. 605-615.
9. Dang, H., Zhao, Y., "CFD Modeling and Experimental Verification of a Single-stage Coaxial Stirling-type Pulse Tube Cryocooler Without Either Double-inlet Or Multi-bypass Operating at 30–35 K Using Mixed Stainless Steel Mesh Regenerator Matrices," *Cryogenics*, 78 (2016), pp. 40-50.
10. Rout, S.K., Gupta, A.K., Choudhury, B.K., Sahoo, R.K. and Sarangi, S.K., "Influence of Porosity on the Performance of a Pulse Tube Refrigerator: a CFD Study," *Procedia Engineering*, 51 (2013), pp. 609-616.
11. Cha, J.S., Ghiaasiaan, S.M. and Kirkconnell, C.S., "Oscillatory Flow in Microporous Media Applied in Pulse – Tube and Stirling – Cycle Cryocooler Regenerators," *Experimental Thermal and Fluid Science*, 32(6) (2008), pp. 1264-1278.